Bioinspired Oil Strider Floating at the Oil/Water Interface Supported by Huge Superoleophobic Force

Xueli Liu,[†,‡] Jun Gao,[†,‡] Zhongxin Xue,[†,‡] Li Chen,[†,‡] Ling Lin,[†,‡] Lei Jiang,[†] and Shutao Wang[†,*]

[†]Beijing National Laboratory for Molecular Sciences, Key Laboratory of Organic Solids, Institute of Chemistry, Chinese Academy of Sciences, Beijing 100190, P. R. China and [‡]Graduate School of Chinese Academy of Sciences, Beijing 100049, P. R. China

ABSTRACT Oil pollution to aquatic devices, especially to those oil-cleaning devices and equipment-repairing robots during oil spill accidents, has drawn great attention and remains an urgent problem to be resolved. Developing devices that can move freely in an oil/water system without contamination from oil has both scientific and practical importance. In nature, the insect water strider can float on water by utilizing the superhydrophobic supporting force received by its legs. Inspired by this unique floating phenomenon, in this article, we designed a model device named "oil strider" that could float stably at the oil/water interface without contamination by oil. The floating capability of the oil strider originated from the huge underwater superoleophobic supporting force its "legs" received. We prepared the micro/nanohierarchical structured copper-oxide-coated copper wires, acting as the artificial legs of oil strider, by a simple base-corrosion process. The surface structures and hydrophilic chemical components of the coatings on copper wires induced the huge superoleophobic force at the oil/water interface, to support the oil strider from sinking into the oil. Experimental results and theoretical analysis demonstrate that this supporting force is mainly composed of three parts: the buoyancy force, the curvature force, and the deformation force. We anticipate that this artificial oil strider will provide a guide for the design of smart aquatic devices that can move freely in an oil/water system with excellent oil repellent capability, and be helpful in practical situations such as oil handling and oil spill cleanup.

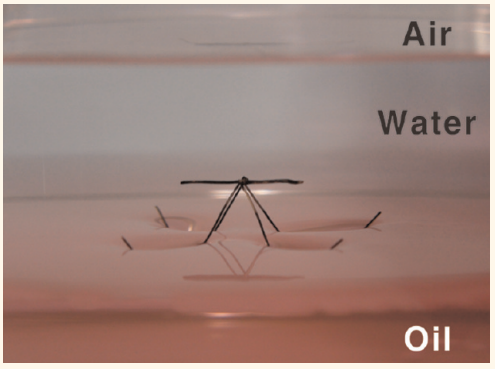

KEYWORDS: aquatic devices · copper materials · interfaces · micro/nanostructures · oil-repellent surfaces · superoleophobic force · underwater superoleophobicity

Oil pollution has drawn worldwide attention as the leakage of crude oil at the surface or bottom of the sea frequently occurred in recent years.[1,2] Besides the destruction to the environment, the contamination of oil, especially suspended oil[1] to aquatic devices, has caused non-negligible economic losses. In addition, oil pollution also affects and hinders the normal operation of oil-cleaning devices and equipment-repairing miniature robots. However, these tough problems still remain unresolved. It is necessary and urgent to develop aquatic devices that can move freely in an oil/water system with excellent oil-repellent capability, to better face the severe oil pollution crisis.

Nature always gives us inspirations to design functional interfaces with special wettability.[3−8] For example, learning from the self-cleaning lotus leaf, superhydrophobic surfaces with low hysteresis of sliding angle have been fabricated successfully.[9] In addition, the directional water-adhesive wings of a butterfly,[10] the antifogging eyes of a mosquito,[11] and the highly adhesive foot of a gecko, [12] *etc.* have also been studied for developing smart interfacial materials and functional devices. These phenomena give us abundant clues to realize special wettability on solid surfaces through the cooperation between surface chemical components and micro/nanohierarchical structures.[13] Following this principle, in-air superoleophobic surfaces can also be created, such as super oil-repellent aluminum plates,[14] super "amphiphobic" aligned carbon nanotube films[15] and polymeric coatings,[16] superoleophobic surfaces with re-entrant surface curvature,[17] self-healing superoleophobic surfaces,[18] superoleophobic transparent surfaces with inverse-trapezoidal microstructures,[19] and superoleophobic coatings with ultralow sliding angles.[20] Although these in-air superoleophobic surfaces show their potential values in various industrial applications, they are not ideal to be used in water, as water generally induces a loss of superoleophobicity.[21−23] Facing this cumbersome situation, scientists again discovered another ingenious way out in nature. By mimicking the skin of the underwater self-cleaning fish, a novel superoleophobic and low adhesive water/solid interface has been

* Address correspondence to stwang@iccas.ac.cn.

Received for review April 8, 2012 and accepted May 19, 2012.

Published online May 19, 2012
10.1021/nn301550v

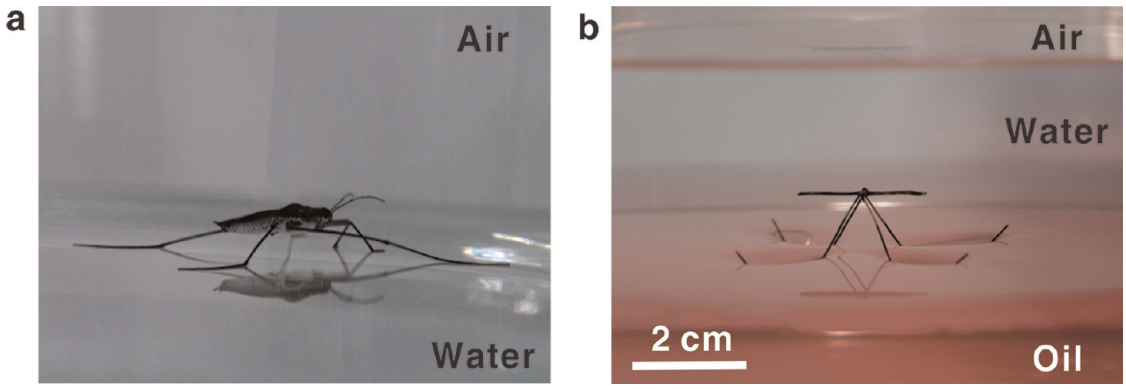

Figure 1. Illustration of the model device oil strider staying at the oil/water interface. (a) A water strider staying at the interface of water/air. (b) The artificial oil strider staying at the interface of oil/water. The legs of the oil strider are copper-oxide-coated copper wires. Crescent-shaped meniscuses are generated around the legs. The oil used is 1,2-dichloroethane. Oil red is used to dye the oil pink.

developed,[24] showing superiority for underwater oil-repellent surfaces. Several underwater superoleophobic surfaces have then been fabricated for their applications in areas such as antibiofouling[25] and antioil-contamination,[26] as well as oil/water separation.[27] But how to expand this new kind of underwater superoleophobic surfaces to smart aquatic devices that can move freely in oil/water system has not been explored up to now.

The water strider is a famous insect that can stand effortlessly and run quickly on water in atmosphere (Figure 1a). It has aroused increasing interest to understand the physical mechanism behind its capability of floating at the water/air interface. Physicists and engineering scientists have done extensive research from the hydrodynamic aspects.[28−31] Caponigro and Eriksen have systematically revealed the two kinds of movements a water strider performs and the different roles of its three kinds of legs in achieving these movements.[28] Hu *et al*. have observed the swirling vortices that the water strider's legs created in order to carry momentum beneath the surface of the water,[29] and demonstrated the two kinds of forces that support the legs: the curvature force and the buoyancy force.[29,31] Recently, chemical scientists have dug more deeply to show that it was the micro/nanohierarchical structures together with hydophobic wax on the water strider's legs that made the legs superhydrophobic.[32−34] This superhydrophobicity induced a strong superhydrophobic force received by the legs at the water/air interface to support its body floating on water.[32] Taking advantage of this supporting force, several artifical models have been developed with superhydrophobic "legs", to realize smart on-water devices with advanced functions such as drag reduction and quick propulsion. For example, Zhang's group have created a self-propelling model on water;[35,36] Saunders *et al*. have fabricated a metallic "pond skater";[37] Hu *et al*.,[38] Shi *et al*.,[39] and Pan *et al*.[40] have also designed separately aritifical water strider-like models. Inspried by this biomimic ideology, we wonder whether this floating mechanism of water strider at the water/air interface can be extended to the oil/water interface, to help in the design of smart devices that are supported from the oil/water interface rather than be polluted by oil?

In this article, we have fabricated underwater superoleophobic copper wires by a simple base-corrosion process. Using these as-prepared wires as the "legs", we have created successfully a model device named "oil strider" (Figure 1b) to prove the feasibility of artificial devices that can move freely at the oil/water interface without oil contamination. The copper wires are coated by micro/nanohierarchical structured copper oxide. This surface structure together with the hydrophilicity of copper oxide induced the huge superoleophobic force, to float the oil strider at the oil/water interface. This huge superoleophobic supporting force probably originates from three main forces: the buoyancy force, the curvature force, and the deformation force. The design of this artificial oil strider provides a strategy to fabricate novel aquatic devices with oil-repellent capability. It would bring promising applications in scientific research and real life, such as drag-reducing and quick propulsion techniques.

RESULTS AND DISCUSSION

As copper is one kind of the engineering materials that are used for aquatic devices and equipments, and copper wires with different diameters can be gotten more easily for the proof-of-concept study, we chose copper to design the model device oil strider. In addition, micro/nanoscaled structures can be easily created on copper surfaces by a simple base-corrosion process. The diameter of the copper wires used for the oil strider's legs was 280 μm, which approximated the average diameter of an adult water strider's legs.[41] The copper wires were bent to three parts, the middle part was about 15 mm while the tip was about 4 mm. Angles between the adjacent two parts of the wire both were 135° (Figure 1b).[38,41,42] These copper wires

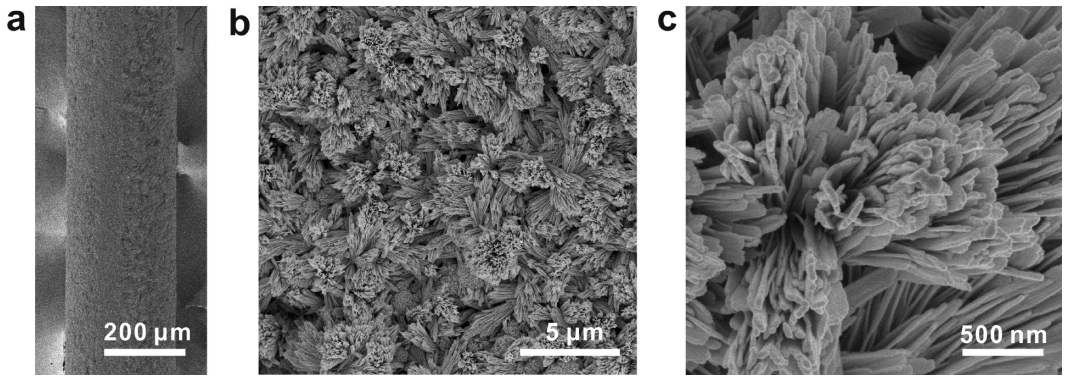

Figure 2. Typical SEM images of the as-prepared copper wires: (a) macroscopically rough surface morphology of the wire (280 μm in diameter); (b) flower-like microclusters at the surface of the wire; (c) the microclusters are composed of nanopetals.

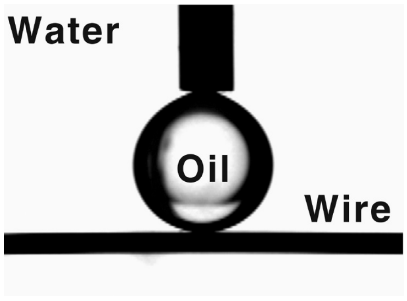

Figure 3. Underwater superoleophobicity of the as-prepared copper wires. Photograph shows an oil droplet (3 μL) on the copper wire (280 μm in diameter). The contact angle (CA) was 164.2 $\pm$ 3.1°. The result was similar to that of other copper wires with different diameters (120, 500, 800, and 1000 μm). Note that this kind of CA is measured on the columnar wire substrate, and the contact between oil droplet and wire is on a line.

were then immersed in aqueous ammonia (pH = 10.5) to generate rough black coatings on them (Figure 2a). X-ray photoelectron spectroscopy (XPS) and X-ray diffraction (XRD) results demonstrate that this coating is composed of copper oxide (see Supporting Information Figure S1).[43−45] This copper-oxide coating was constructed by flower-like microclusters (about 1−5 μm in diameter, Figure 2b) with nanopetals (about 100 nm in width, Figure 2c). Underwater oleophobicity of the as-prepared copper wires was then measured using contact angle (CA) instrument. A droplet of oil (1,2-dichloroethane, 3 μL) was hung on a needle to contact the copper wire. The CA of oil droplet on the columnar wire substrate at the time they just contacted was 164.2 $\pm$ 3.1° (Figure 3). In this situation, the oil droplet contacted the wire on a line. Besides, we also measured the CA of oil droplet on the flat copper sheet, which was 164.8 $\pm$ 5.0°. These results demonstrate that the copper-oxide coated wires are underwater superoleophobic. In addition, when the wire was moved up to squeeze the oil droplet and then moved down to leave, there was almost no deformation of the droplet and no oil residual left on the wire (see Supporting Information Figure S2). This suggests that the hysteresis of the contact angle is very small and the adhesion between oil and wire is extremely low.[35] The underwater superoleophobicity of the as-prepared copper wires resulted from the synergistic effect of chemical components and micro/nanohierarchical structures of the copper-oxide coating. Hydrophilicity of copper oxide induces water to be trapped in the interstice of micro/nanohierarchical structures. A minimized oil/solid contact area gives rise to superoleophobicity and low oil adhesion of the wires. This underwater superoleophobicity can also be achieved by combining other hydrophilic materials (such as solid oxides, hydroxides, and other oxygenated compounds) with surface micro/nanohierarchical structures.

After we put the oil strider on the underwater-oil surface, it could stay at the oil/water interface, as shown in Figure 1b. The oil was 1,2-dichloroethane. Its density is larger than water so it lies at the bottom when mixed with water. To distinguish water with oil and make the interface clear, we used oil red to dye the oil pink. The oil strider could stand on the underwater-oil surface although the density of copper is larger than that of 1,2-dichloroethane. The crescent-shaped meniscus generated around the legs of the oil strider (Figure 1b) was similar to that of the water strider. These results suggest that the underwater superoleophobicity of copper wires draws a huge superoleophobic force to support the body of the oil strider staying at the oil/water interface without sinking into oil.

The received supporting force of the as-prepared copper wires at the oil/water interface was systematically studied by measuring the changes of received force of wires with different diameters when they passed through the oil/water interface. Copper wires of different diameters (120, 280, 500, 800, and 1000 μm) were used in this experiment. To simplify the research system, the shape of the copper wires was abstracted to an "L" shape with a right angle. The short part of the as-prepared "L" wire was about 2 cm and the long part was 4 cm. The surface structures of the four kinds of wires (with 120, 500, 800, and 1000 μm in diameter) after corrosion are shown in Supporting Information

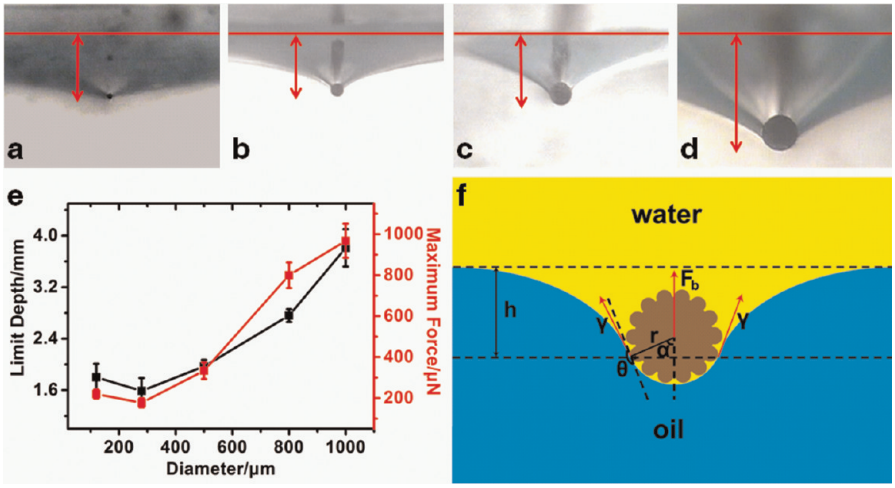

Figure 4. Analysis of the supporting force received by the as-prepared copper wires when they pass through the oil/water interface. (a–d) Photographs show the limit depths of copper wires with different diameters when they pass through the interface. The corresponding diameter of the wires is 120 (a), 280 (b), 500 (c), and 800 μm (d). (e) Graph shows the relationship between the diameter of the wires and the limit depth, the maximum force received. (f) Schematic illustration of the cross section view of micro/nanohierarchical structured copper wires when passing through the oil/water interface, *r* represents the radius of the wire and in this scheme, it starts from the center of the wire to the point where the oil/water interface is separated by the wire. γ is the interfacial tension of oil/water interface. α is the angle between the vertical line and *r*, and θ is the angle between the tangent line of the oil/water interface and the tangent line of the wire at the point where the oil/water interface is separated by the wire. Micro/nanohierarchical structures on copper wires trap water and reduce the oil/wire contact area. This results in underwater superoleophobicity of copper wires and the maximum θ, contributing to the huge F_s.

Figure S3. They were all composed by micro/nanohierarchical structures. Although the surface morphologies of them were not completely the same, these wires were all underwater superoleophobic. The CA of oil was correspondingly 172.7 ± 1.1° (for copper wire 120 μm in diameter); 167.7 ± 3.5° (for copper wire 500 μm in diameter); 168.9 ± 4.1° (for copper wire 800 μm in diameter); and 168.2 ± 2.3° (for copper wire 1000 μm in diameter). (Note that all these CAs were measured on columnar wire substrates.) We used a highly sensitive microelectromechanical balance system (DataPhysics DCAT 11, dynamic contact angle meters and tensiometers, Limit of Detection: 1 μN) to detect the received force of the "L" wires. A CCD camera was used to record the related images simultaneously. The oil/water system was first placed in a glass container below the balance. During the force measurement procedure, the long part was fixed into the holder of the balance to make the short part horizontal to the oil/water interface. The short part was first immersed into the water layer. Then the oil/water interface moved upward at a rate of 50 μm s^{-1} until an immersion depth of 8 mm was reached. It then moved down at the same rate to the original position. The short part of the wire first contacted with the oil/water interface and then penetrated the interface and into the oil. In this measurement cycle, the limit depth and the maximum force that the wires got before penetrating the interface were recorded by the device, as the initial position and original received force of the wires were both set to zero.

Figure 4 panels a–d show the relative positions of the four wires with diameters of 120, 280, 500, and 800 μm recorded by the CCD camera in the cross-sectional view just before they penetrate the oil/water interface. Figure 4e shows the relationships between the diameter of the copper wires and the maximum force received and the limit depths are concluded. It is noteworthy that they are not completely positively related. There exists a minimum in both the limit depth and the received maximum force when the diameter of copper wire is 280 μm. The mechanism behind this force regularity was then analyzed and modeled according to previous studies.[29,36] Figure 4f shows the force analysis of the wire at the oil/water interface. The total received support force F_s includes three parts, as described in eq 1.

$$F_s = F_b + F_c + F_d \quad (1)$$

$$F_b = \pi\rho_w g r^2 + \left(\alpha - \sin\alpha\cos\alpha + 2\frac{h\sin\alpha}{r}\right)(\rho_o - \rho_w)gr^2 \quad (2)$$

$$F_c = -2\gamma\cos(\alpha+\theta) \quad (3)$$

where F_b is the buoyancy force, F_c is the curvature force, and F_d is the deformation force. ρ_w represents the density of water, while ρ_o represents the density of oil. *r* is the radius of copper wire, and γ is the interfacial tension of oil/water interface. θ represents the contact angle of oil droplet on copper wire. *h* and α are two quantities defined to help the calculation with no physical meanings, and are shown more clearly in Figure 4f).

F_b is related to wire radius *r* and r^2, and increases as *r* increases, as shown in eq 2. F_c is related to interfacial

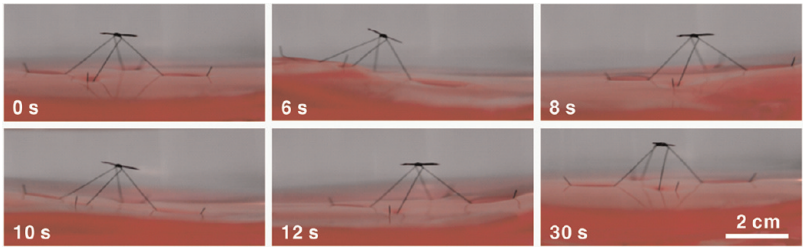

Figure 5. The dynamic stability of the oil strider's floating at the oil/water interface. As the interface waves, the oil strider moves up and down but never sinks into the oil layer below. When the wave goes to calm at 30 s, the oil strider still stably stands at the interface. To distinguish the oil/water interface, the oil is dyed pink.

tension, its value will not change when the material is the same in one system (γ represents the interfacial tension of oil/water interface), as concluded in eq 3. The deformation force F_d is mainly related to wr, r^{-3}, and r^{-4} (w is the deflection of the copper wire), which is consistent with the report of Zhang's group.[36] As r decreases, F_d increases. When the diameter of copper wire is 120 μm, the wire is softer and is more easily bent than wire with 280 μm diameter. F_d becomes larger and determines the value of the totally received force. Thus, both the maximum force and the limit depth of wire with a diameter of 120 μm are larger than that of the wire with diameter of 280 μm (Figure 4a,b,e). When the diameter of the wire is larger than 280 μm, the deformation of the wire becomes too little to be considered. Therefore, F_d can be ignored and F_b begins playing the important role. The total force increases as the diameter increases (Figure 4b–e). Thus, the minimum force and limit depth in this system are reached when the diameter is 280 μm. In addition, surface micro/nanohierarchical structures of those copper wires are very important for reaching the huge supporting forces. When the surface structures turned from smooth to rough, both the limit depth and F_s increased (see Supporting Information, Figures S4 and S5). This is because surface structures influence the underwater oleophobicity of the copper wires. As shown in eq 3, F_c is related to the contact angle θ of the oil droplet on copper wire. When θ increases, F_c increases. Surface micro/nanohierarchical structures induced the underwater superoleophobicity of those copper wires as well as the maximum θ, thus resulting in the maximum F_c and contributing to the huge supporting force F_s.

The force analysis helps us to understand the physical mechanism behind the oil strider's capability to float at the oil/water interface. In fact, for a model device, gravity also influences its floating capability. For a copper wire floating at the oil/water interface, there exists the limit of floating when $F_b + F_c = mg$ (there is no F_d as the copper wire freely floats at the interface alone). The calculation result shows that the limit diameter of the wire is about 900–1000 μm in our system. We also demonstrated this by doing the experiment. We chose two as-prepared copper wires, one was 800 μm and the other was 1000 μm, and put them at the oil/water interface. The wire with diameter of 800 μm could float at the interface while the one with diameter of 1000 μm sank down. Similarly, for the oil strider, only when its body gravity is smaller than the total supporting force that its four legs received, can it keep the free-floating capability at the interface. By a measurement of the received supporting force of the copper wires, the limit gravity of the oil strider can be deduced. Therefore, it is necessary to take gravity into consideration for device design in further practical applications.

The stability of the oil strider floating at the oil/water interface was also tested in our experiment. After the oil strider was put on the underwater-oil surface, we rocked the container to wave the oil/water interface. As the interface waved, the oil strider rose and fell, as shown in Figure 5. In the whole process from the start to the calm of waves in 30 s, the oil strider floated up and down but never penetrated the interface into the oil layer. Finally at the end of the time, the oil strider still stably stood on the oil surface. In the experiment, the oil strider could stay at the interface for at least 3 h. After the experiment, the oil strider was taken out from the oil/water system, without any oil residual adhered on its legs. After about three month's storage, this oil strider still kept the stably free-floating capability. These results further indicate that the artificial legs have stable underwater superoleophobicity.

CONCLUSIONS

In summary, inspired by the unique floating capability of a water strider, we successfully fabricated a model device, an oil strider capable of free floating at the oil/water interface, supported by the huge underwater superoleophobic force its artificial copper-wire legs received. Micro/nanohierarchical structures and hydrophilic components of the copper-oxide coatings on the as-prepared copper-wire legs resulted in this huge and stable underwater superoleophobic force at the oil/water interface. This oil strider could stably float at the oil/water interface without contamination by oil. The concept of this model device can also be applied to other engineering metal materials such as Fe, Al,

and alloys. We anticipate that this research can give enlightenment to the development of drag-reducing materials, underwater-oil vent devices, underwater safeguard robots, underwater-oil-cleaning devices, and other aquatic smart devices with superior oil-repellent capability.

MATERIALS AND METHODS

Fabrication and Characterization of Rough Copper-Oxide Coatings on Copper Wires. In brief, copper wires were sequentially cleaned in acetone, ethanol, and deionized water by ultrasonic means, each for 10 min, to get rid of contaminants and the insulating barrier on wires. The wires were then soaked in 0.1 M HCl (aq) to remove the outside oxidation layer. After being rinsed with deionized water three times, the wires were immersed in aqueous ammonia at pH 10.5 for about 36 h at ambient temperature to get the black copper-oxide-coated surfaces, and finally rinsed and stored in dry containers.

A field-emission scanning electron microscope (JSM-6700F, Japan) was used for characterizing the morphology of the as-prepared copper wire surfaces. X-ray photoelectron spectroscopy (XPS) and X-ray diffraction pattern (XRD) data were collected using aqueous ammonia corroded copper sheets prepared at the same experiment parameters as copper wires, to facilitate the analysis. XPS data were obtained with an ESCALab220i-XL electron spectrometer from VG Scientific using 300 W MgKα radiation. The base pressure was about 3×10^{-9} mbar. XRD patterns were collected with a Mac Science MXP-AHF18 X-ray diffractometer using Cu Kα radiation. Contact angles were measured by an OCA20 contact angle system (DataPhysics, Germany).

Measurement of the Received Supporting Force and the Limit Depth of the As-Prepared Copper Wires. The corresponding copper wires were first bent to an "L" shape before the corrosion step to avoid the probable damage of the surface structures during the subsequent measurement process. The long part of the "L" shape wire was about 4 cm, and the short part was about 2 cm. During the measurement, the long part was fixed to the holder on the high-sensitivity micro-electromechanical balance (Data-Physics DCAT 11, dynamic contact angle meters and tensiometers, Limit of Detection: 1 μN), to make the short part parallel to the oil/water interface. The oil/water system was placed within a glass container put right below the holder. The water was Mill-Q grade, and the oil was 1,2-dichloroethane. The density of the oil is larger than water so that it lies below the water phase, as they are immiscible. After the wire was immersed in the water phase, the oil/water interface moved upward at a rate of 50 μm s^{-1} until a preinstalled immersion depth of 8 mm was reached, and then moved down at the same rate to the original position. The start received force and immersion depth of the wire in the water phase were all set to zero before the interface began to move. The wire first contacted with the interface, then reached a limit and penetrated the interface, and finally went into the oil phase. The received force and the relative immersion position of the copper wire were collected by the balance system and the entire process was also recorded by the CCD camera.

Conflict of Interest: The authors declare no competing financial interest.

Acknowledgment. The authors are grateful for financial support by the National Research Fund for Fundamental Key Projects (2012CB933800, 2009CB930404, 2010CB934700, 2011CB935700, 2012CB933200), National Natural Science Foundation (21175140, 20974113, 21071148, 20920102036, 21121001, 91127025), and the Key Research Program of the Chinese Academy of Sciences (KJZD-EW-M01).

Supporting Information Available: X-ray photoelectron spectroscopy and X-ray diffraction analysis of copper-oxide coated copper wires; measurement results that demonstrate the low adhesion between oil droplet and the as-prepared copper wires; SEM characterization of the copper-oxide-coated copper wires with diameters of 120, 500, 800, and 1000 μm; and the influence of surface morphology to the received supporting force and limit depth of copper wires when they pass through the oil/water interface. This material is available free of charge *via* the Internet at http://pubs.acs.org.

REFERENCES AND NOTES

1. Kingston, P. F. Long-Term Environmental Impact of Oil Spills. *Spill Sci. Technol. Bull.* **2002**, *7*, 53–61.
2. Gossen, L. P.; Velichkina, L. M. Environmental Problems of the Oil-and-Gas Industry. *Pet. Chem.* **2006**, *46*, 67–72.
3. Wong, T. S.; Kang, S. H.; Tang, S. K. Y.; Smythe, E. J.; Hatton, B. D.; Grinthal, A.; Aizenberg, J. Bioinspired Self-Repairing Slippery Surfaces with Pressure-Stable Omniphobicity. *Nature* **2011**, *477*, 443–447.
4. Aussillous, P.; Quéré, D. Liquid Marbles. *Nature* **2001**, *411*, 924–927.
5. Zheng, Y. M.; Bai, H.; Huang, Z. B.; Tian, X. L.; Nie, F. Q.; Zhao, Y.; Zhai, J.; Jiang, L. Directional Water Collection on Wetted Spider Silk. *Nature* **2010**, *463*, 640–643.
6. Bhushan, B. Biomimetics: Lessons from Nature—An Overview. *Phil. Trans. R. Soc. A* **2009**, *367*, 1445–1486.
7. Barthlott, W.; Schimmel, T.; Wiersch, S.; Koch, K.; Brede, M.; Barczewski, M.; Walheim, S.; Weis, A.; Kaltenmaier, A.; Leder, A.; *et al*. The Salvinia Paradox: Superhydrophobic Surfaces with Hydrophilic Pins for Air Retention Under Water. *Adv. Mater.* **2010**, *22*, 2325–2328.
8. Nosonovsky, M.; Bhushan, B. Biomimetic Superhydrophobic Surfaces: Multiscale Approach. *Nano Lett.* **2007**, *7*, 2633–2637.
9. Feng, L.; Li, S. H.; Li, Y. S.; Li, H. J.; Zhang, L. J.; Zhai, J.; Song, Y. L.; Liu, B. Q.; Jiang, L.; Zhu, D. B. Super-Hydrophobic Surfaces: From Natural to Artificial. *Adv. Mater.* **2002**, *14*, 1857–1860.
10. Zheng, Y. M.; Gao, X. F.; Jiang, L. Directional Adhesion of Superhydrophobic Butterfly Wings. *Soft Matter* **2007**, *3*, 178–182.
11. Gao, X. F.; Yan, X.; Yao, X.; Xu, L.; Zhang, K.; Zhang, J. H.; Yang, B.; Jiang, L. The Dry-Style Antifogging Properties of Mosquito Compound Eyes and Artificial Analogues Prepared by Soft Lithography. *Adv. Mater.* **2007**, *19*, 2213–2217.
12. Hansen, W. R.; Autumn, K. Evidence for Self-Cleaning in Gecko Setae. *Proc. Natl. Acad. Sci. U.S.A.* **2005**, *102*, 385–389.
13. Xia, F.; Jiang, L. Bio-Inspired, Smart, Multiscale Interfacial Materials. *Adv. Mater.* **2008**, *20*, 2842–2858.
14. Tsujii, K.; Yamamoto, T.; Onda, T.; Shibuichi, S. Super Oil-Repellent Surfaces. *Angew. Chem., Int. Ed.* **1997**, *36*, 1011–1012.
15. Li, H. J.; Wang, X. B.; Song, Y. L.; Liu, Y. Q.; Li, Q. S.; Jiang, L.; Zhu, D. B. Super-"Amphiphobic" Aligned Carbon Nanotube Films. *Angew. Chem., Int. Ed.* **2001**, *40*, 1743–1746.
16. Xie, Q. D.; Xu, J.; Feng, L.; Jiang, L.; Tang, W. H.; Luo, X. D.; Han, C. C. Facile Creation of a Super-Amphiphobic Coating Surface with Bionic Microstructure. *Adv. Mater.* **2004**, *16*, 302–305.
17. Tuteja, A.; Choi, W.; Ma, M. L.; Mabry, J. M.; Mazzella, S. A.; Rutledge, G. C.; McKinley, G. H.; Cohen, R. E. Designing Superoleophobic Surfaces. *Science* **2007**, *318*, 1618–1622.
18. Wang, H.; Xue, Y.; Ding, J.; Feng, L.; Wang, X.; Lin, T. Durable, Self-Healing Superhydrophobic and Superoleophobic Surfaces from Fluorinated-Decyl Polyhedral Oligomeric Silsesquioxane and Hydrolyzed Fluorinated Alkyl Silane. *Angew. Chem., Int. Ed.* **2011**, *50*, 11433–11436.
19. Im, M.; Im, H.; Lee, J. H.; Yoon, J. B.; Choi, Y. K. A Robust Superhydrophobic and Superoleophobic Surface with

Inverse-Trapezoidal Microstructures on a Large Transparent Flexible Substrate. *Soft Matter* **2010**, *6*, 1401–1404.
20. Zhang, J. P.; Seeger, S. Superoleophobic Coatings with Ultralow Sliding Angles Based on Silicone Nanofilaments. *Angew. Chem., Int. Ed.* **2011**, *50*, 6652–6656.
21. Jung, Y. C.; Bhushan, B. Wetting Behavior of Water and Oil Droplets in Three-Phase Interfaces for Hydrophobicity/philicity and Oleophobicity/philicity. *Langmuir* **2009**, *25*, 14165–14173.
22. Jin, M. H.; Wang, J.; Yao, X.; Liao, M. Y.; Zhao, Y.; Jiang, L. Underwater Oil Capture by a Three-Dimensional Network Architectured Organosilane Surface. *Adv. Mater.* **2011**, *23*, 2861–2864.
23. Hejazi, V.; Nosonovsky, M. Wetting Transitions in Two-, Three-, and Four-Phase Systems. *Langmuir* **2012**, *28*, 2173–2180.
24. Liu, M. J.; Wang, S. T.; Wei, Z. X.; Song, Y. L.; Jiang, L. Bioinspired Design of a Superoleophobic and Low Adhesive Water/Solid Interface. *Adv. Mater.* **2009**, *21*, 665–669.
25. Chen, L.; Liu, M. J.; Bai, H.; Chen, P. P.; Xia, F.; Han, D.; Jiang, L. Antiplatelet and Thermally Responsive Poly(*N*-isopropylacrylamide) Surface with Nanoscale Topography. *J. Am. Chem. Soc.* **2009**, *131*, 10467–10472.
26. Lin, L.; Liu, M. J.; Chen, L.; Chen, P. P.; Ma, J.; Han, D.; Jiang, L. Bio-Inspired Hierarchical Macromolecule-Nanoclay Hydrogels for Robust Underwater Superoleophobicity. *Adv. Mater.* **2010**, *22*, 4826–4830.
27. Xue, Z.; Wang, S.; Lin, L.; Chen, L.; Liu, M.; Feng, L.; Jiang, L. A Novel Superhydrophilic and Underwater Superoleophobic Hydrogel-Coated Mesh for Oil/Water Separation. *Adv. Mater.* **2011**, *23*, 4270–4273.
28. Caponigro, M. A.; Eriksen, C. H. Surface Film Locomotion by Water Strider, Gerris-Remigis Say. *Am. Midl. Nat.* **1976**, *95*, 268–278.
29. Hu, D. L.; Chan, B.; Bush, J. W. M. The Hydrodynamics of Water Strider Locomotion. *Nature* **2003**, *424*, 663–666.
30. Dickinson, M. Animal Locomotion: How to Walk on Water. *Nature* **2003**, *424*, 621–622.
31. Hu, D. L.; Bush, J. W. M. Meniscus-Climbing Insects. *Nature* **2005**, *437*, 733–736.
32. Gao, X. F.; Jiang, L. Water-Repellent Legs of Water Striders. *Nature* **2004**, *432*, 36–36.
33. Feng, X. Q.; Gao, X. F.; Wu, Z. N.; Jiang, L.; Zheng, Q. S. Superior Water Repellency of Water Strider Legs with Hierarchical Structures: Experiments and Analysis. *Langmuir* **2007**, *23*, 4892–4896.
34. Watson, G. S.; Cribb, B. W.; Watson, J. A. Experimental Determination of the Efficiency of Nanostructuring on Non-wetting Legs of the Water Strider. *Acta Biomater.* **2010**, *6*, 4060–4064.
35. Shi, F.; Wang, Z. Q.; Zhang, X. Combining a Layer-by-Layer Assembling Technique with Electrochemical Deposition of Gold Aggregates to Mimic the Legs of Water Striders. *Adv. Mater.* **2005**, *17*, 1005–1009.
36. Shi, F.; Niu, J.; Liu, J. L.; Liu, F.; Wang, Z. Q.; Feng, X. Q.; Zhang, X. Towards Understanding Why a Superhydrophobic Coating Is Needed by Water Striders. *Adv. Mater.* **2007**, *19*, 2257–2261.
37. Larmour, I. A.; Bell, S. E. J.; Saunders, G. C. Remarkably Simple Fabrication of Superhydrophobic Surfaces Using Electroless Galvanic Deposition. *Angew. Chem., Int. Ed.* **2007**, *46*, 1710–1712.
38. Jiang, L.; Yao, X.; Li, H. X.; Fu, Y. Y.; Chen, L.; Meng, Q.; Hu, W. P. "Water Strider" Legs with a Self-Assembled Coating of Single-Crystalline Nanowires of an Organic Semiconductor. *Adv. Mater.* **2010**, *22*, 376–379.
39. Wu, X. F.; Shi, G. Q. Production and Characterization of Stable Superhydrophobic Surfaces Based on Copper Hydroxide Nanoneedles Mimicking the Legs of Water Striders. *J. Phys. Chem. B* **2006**, *110*, 11247–11252.
40. Zhang, X.; Zhao, J.; Zhu, Q.; Chen, N.; Zhang, M.; Pan, Q. Bioinspired Aquatic Microrobot Capable of Walking on Water Surface Like a Water Strider. *ACS Appl. Mater. Interfaces* **2011**, *3*, 2630–2636.
41. Yao, X.; Xu, L.; Jiang, L. Fabrication and Characterization of Superhydrophobic Surfaces with Dynamic Stability. *Adv. Funct. Mater.* **2010**, *20*, 3343–3349.
42. Vella, D. Floating Objects with Finite Resistance to Bending. *Langmuir* **2008**, *24*, 8701–8706.
43. Pei, M. D.; Wang, B.; Li, E.; Zhang, X. H.; Song, X. M.; Yan, H. The Fabrication of Superhydrophobic Copper Films by a Low-Pressure-Oxidation Method. *Appl. Surf. Sci.* **2010**, *256*, 5824–5827.
44. Brookshier, M. A.; Chusuei, C. C.; Goodman, D. W. Control of CuO Particle Size on SiO_2 by Spin Coating. *Langmuir* **1999**, *15*, 2043–2046.
45. Scrocco, M. Satellite Structure in the X-ray Photoelectron-Spectra of CuO and Cu_2O. *Chem. Phys. Lett.* **1979**, *63*, 52–56.